Macromolecules
ARTICLE

Macromolecules **2009**, *42*, 4719–4727 **4719**
DOI: 10.1021/ma900645f

Rheology, Processing, Tensile Properties, and Crystallization of Polyethylene/Carbon Nanotube Nanocomposites

J. F. Vega and J. Martínez-Salazar*

Departamento de Física Macromolecular, Instituto de Estructura de la Materia, CSIC, Serrano 113 bis, 28006 Madrid, Spain

M. Trujillo, M. L. Arnal, and A. J. Müller*

Grupo de Polímeros USB, Departamento de Ciencia de los Materiales, Universidad Simón Bolívar, Apartado 89000, Caracas 1080-A, Venezuela

S. Bredeau and Ph. Dubois

Service des Matériaux Polymerès et Composites SMPC, Center of Research and Innovation in Materials & Polymers CIRMAP, University of Mons, Place du Parc 20, B-7000 Mons, Belgium.

Received March 25, 2009; Revised Manuscript Received May 9, 2009

ABSTRACT: A nanocomposite sample was prepared by melt mixing a high density polyethylene (HDPE) with an in situ polymerized HDPE/multi wall carbon nanotube (MWNT) masterbatch. The nanocomposite had an approximate content of 0.52 wt % MWNT. Rheological, thermal, and mechanical properties were investigated for both neat HDPE and nanocomposite. The nanocomposite, when compared to the neat polymer, exhibits lower values of viscosity, shear modulus and shear stress in extrusion and a concurrent delay of the distortion regimes to higher shear stresses and rates. The nanocomposite presents also improved dimensional stability after processing, and lower values of the melt strength, draw ratio and viscosity in elongational flow. This behavior has been observed in composites in which an adsorption of a fraction (that with the highest molecular weight or relaxation time) of the polymer chains is considered. Furthermore, the enhancement in the crystallization kinetics, probed by rheometry and DSC, suggests that the carbon nanotubes act as nucleating agents for the polymeric chains. Additionally, the presence of adsorbed chains does not only influence the molten state but also induces interesting effects in the mechanical properties of the polymer. As a result, an increase of up to 100% in elastic modulus was observed in the HDPE/MWNT nanocomposite without losing the ductility present in neat HDPE.

1. Introduction

The preparation of polymer/carbon nanotube (CNT) composites has been an area of growing scientific interest since the exceptional properties of CNT may extend the applications and final uses of polymeric materials. These nanocomposites may find applications as structural materials, due to their low density, increased mechanical properties and electrical conduction, and also as selectively permeable membranes in electromagnetic induction shielding.[1] There are two key aspects related to the transfer of the exceptional properties of CNT to polymeric materials. First, the CNT must be homogeneously dispersed throughout the polymer matrix, and second, a degree of interaction between the macromolecular chains and the CNT must be present. Nanotubes, whether bundles of single wall carbon nanotubes (SWNTs) or aggregates of multiwall carbon nanotubes (MWNTs), have a strong tendency to agglomerate, and it is very difficult to separate individual nanotubes during mixing with a polymeric material. Different methods have been developed in order to overcome these difficulties. Solution blending, melt blending, and "in situ" polymerization are widely applied techniques to produce nanotube/polymer composites.[2]

*Corresponding authors. E-mail: (J.M.-S.) jmsalazar@iem.cfmac.csic.es; (A.J.M.) amuller@usb.ve.

The viscoelastic properties of nanotube/polymer composites have both practical and basic importance since they are related to composite processing, dynamics and microstructure. Several theoretical[3−7] and experimental[3] studies have been performed to try to determine how the carbon nanotubes influence the rheological and mechanical behavior of these nanocomposites. Recently, the effects of the aspect ratio[8] and the CNT dispersion[9−12] have been evaluated. Cipriano et al.[9] studied the effect of MWNT aspect ratio (they employed $L/D = 49$ and 150) on the rheological properties of polystyrene (PS)/MWNT nanocomposites. They found larger storage modulus and complex viscosities for the nanocomposites prepared with the 150 aspect ratio. The effect of the interactions between CNT and the matrix has been the subject of several recent studies.[10−13] Seyhan et al.[13] investigated the effect of functionalizing MWNT with amine groups in order to improve their interactions with poly(vinyl ester)s. They found that nanocomposites prepared with 0.3% neat MWNT exhibited a viscous behavior ($G'' > G'$). On the other hand, the nanocomposite with functionalized MWNT of identical composition had a more viscoelastic behavior ($G'' \sim G'$). This can be considered a demonstration that the interactions between the matrix and the filler influence the rheological behavior. A similar result was found by Wu et al.[9] in a poly(L-lactide) (PLLA)/MWNT nanocomposite when the CNT were

Published on Web 05/28/2009

chemically modified. Wu et al. have also prepared CNT nanocomposites employing polybutylene terephtalate (PBT),[14] polycarbonate (PC),[15] and poly(ε-caprolactone) (PCL)[16] matrices. In this last case, they reported percolated networks of nanotubes for 2 and 3% CNT contents. Another result reported by several authors[9−13] is that most nanocomposites prepared with CNT are highly shear thinning without the usual Newtonian plateau at low shear rates that is usually observed for the neat polymer that conforms the matrix.

The general behavior reported in the literature for oscillatory shear rheological measurements at low frequencies is that the linear rheological properties evolve from a liquid-like behavior to a solid-like behavior as the nanotube concentration increases. The application of a power law function to the evolution of properties with nanotube loading data provides a tool to estimate the percolation threshold, corresponding to the onset of solid-like behavior. Additionally, it has been observed that this transition from liquid-like to solid-like behavior can be observed at lower CNT concentrations as the dispersion is improved, or the interaction between the nanofiller and the matrix is stronger or the CNT aspect ratio is larger. In concordance, as with electrical percolation, the rheological percolation is a function of nanotube dispersion (which mainly depends on the method of preparation), aspect ratio, and alignment. Due to these reasons, different values of the percolation threshold can be found in the literature for several types of nanocomposites.[1,17−29] For PS/CNT and PCL/CNT systems, values of 1.0 and 3 wt % have been recently found.[17,23,24] In the case of PC/CNT nanocomposites the values range between 0.25 and 0.75%.[18,25] Even lower values (0.12 wt %) have been found in the case of poly(methyl methacrylate) (PMMA)/CNT systems.[19] Higher values, and in a wider range of compositions between 0.5% and 7.5%, have been reported in the case of polypropylene (PP)/CNT[20,26] and polyethylene (PE)/CNT systems.[21−23] Except for refs 21, 23, and 26, all the reported percolation compositions are well below 2−3% (see also the review in ref 1). Previous works with PE/CNT nanocomposites have reported huge increases in viscosity and storage modulus values with CNT contents.[21,23,30,31]

In this work, the rheological and mechanical properties of PE/MWNT nanocomposites with 0.52 wt % MWNT are studied. These nanocomposites were obtained by melt blending a masterbatch of PE/MWNT prepared by *in situ* polymerization with a commercial polyethylene resin. We believe that the peculiar morphology obtained by "in situ" polymerization, where the PE chains directly grow from the surface of the CNT and are nucleated by them, has strongly influenced the behavior and is responsible for the remarkable results obtained.

2. Materials

The high-density polyethylene (HDPE) employed in this work was a commercial blown film grade prepared by Ziegler−Natta catalysis. Its density is $\rho = 0.955$ g/cm^3 and its melt flow index (190 °C/2.1 kg) = 0.05 dg/min. Its average molar masses are $\overline{M}_n = 12\,500$ and $\overline{M}_w = 230\,000$. This HDPE is a copolymer with a small content of 1-butene as comonomer and has a bimodal molecular weight distribution with a higher molar mass fraction that is larger than its lower one.[32] This HDPE is marketed as Venelene 7000F and was produced in Venezuela by Poliolefinas Internacionales, C.A. POLINTER. In order to prepare the nanocomposite employed here, the described HDPE was melt mixed in an Atlas mini-extruder at 200 °C (and 60 rpm) with 1 wt % of an *in situ* polymerized masterbatch. The masterbatch composition was 43 wt % of PE, 52 wt % of MWNT and 5 wt % of oxidized catalytic residues (mainly alumina). The masterbatch is denoted $PE_{43}M_{52}A_5$, where the subscripts indicate the composition in wt %. The nanocomposite employed in this work (HDPE/1 wt % $PE_{43}M_{52}A_5$) had a final content of 0.52 wt % MWNT. The preparation of the masterbatch has been described in detail elsewhere.[33,34] The *in situ* polymerization process has been designed to produce an optimum dispersion since the PE chains grow directly on the surface of the MWNTs, which contain a previously deposited metallocene catalyst, disaggregating the initially bundle-like entangled MWNTs.[35]

The extrusion was performed employing two types of dies. In one extrusion experiment, a circular die was employed to produce pellets, and in another, a flat die was used to extrude 0.4 mm thick sheets. The sheets were cut with a dog bone shape die and tensile testing specimens were produced. The pellets were compression molded into similarly thick sheets that were also cut into dog bone shaped specimens. Tensile testing was performed in both types of samples, and similar results were obtained, suggesting that the extruded sheets were produced with minimum orientation (a result of the slow pulling rate at the extruder exit and relatively high molding temperature).

3. Experimental Techniques

3.1. Oscillatory Shear Measurements in the Melt and Crystallization. The measurements were performed in a CVO Bohlin torsion rheometer in the linear viscoelastic region at low strain ($\gamma = 10\%$) at different frequencies $\omega = 6 \times 10^{-3}$ to 60 rad·s^{-1}) and a temperature of 160 °C. The influence of MWNT during crystallization of the neat HDPE matrix was also investigated using dynamic rheometry. Compression-molded samples were left inside the rheometer to relax at 180 °C for 1 h. Subsequently, the samples were cooled from 160 °C to T_c at 15 °C/min. At constant strain $\gamma = 0.15\%$ and frequency $\nu = 1$ Hz, isothermal crystallization at different temperatures was followed by measuring the time evolution of the storage modulus G'. The procedure is quite similar to that used in ref 21 for UHMWPE/CNT composites.

3.2. Capillary Flow and Continuous Torsion. The neat HDPE material and the nanocomposite were also subjected to capillary extrusion using a piston-type CEAST Rheoscope 1000. Results of the apparent shear stress, $\sigma_{w,app}$, at different apparent shear rates, $\dot{\gamma}_{app}$, were collected in the range between 10 and 1000 s^{-1} using a 1 mm diameter die capillary with a length/diameter ratio of 20. The melt temperature was maintained in these experiments at 160 °C. Individual extrudate samples were collected. Also nonlinear measurements in the Bohlin CVO stress-controlled rheometer in continuous torsion mode were performed at 160 °C using the cone−plate geometry (25 mm diameter), in order to obtain the shear viscosity, within the shear rate range 0.1−10 s^{-1}.

3.3. Elongational Properties. Samples were melt spun as monofilaments at 160 °C using a melt spinning line adapted to the piston-type CEAST Rheoscope 1000. Extrudates obtained at 24 s^{-1} in the rheometer described above, were stretched with a rotor. The tensile force, F, was measured as the draw ratio v_L/v_0 (v_L is the take up velocity of the rotor; v_0 is the velocity of the extrudate at the exit of the die, 3 mm/s) was increased up to filament rupture.

3.4. Thermal Properties. Differential scanning calorimetry (DSC) was performed with a Perkin-Elmer Pyris 1 instrument calibrated with indium and tin under an ultra high purity nitrogen atmosphere. Sample weights of approximately 5 mg were employed and the samples were encapsulated in aluminum pans and sealed. The crystalline thermal history was erased by heating the samples at 170 °C for 3 min. Cooling and subsequent heating scans were registered at 10 °C/min.

The isothermal crystallization kinetics was also evaluated. Samples were first heated to 170 °C and kept in the melt for 3 min, in order to erase all crystalline thermal history, before they were quenched (at a controlled rate of 60 °C/min) to the chosen isothermal crystallization temperature, T_c. In order to evaluate if the sample was able to crystallize during the previous quenching at 60 °C/min, the sample was immediately heated

after quenching while recording its heating scan at 10 °C/min. For the temperature range evaluated (123.5, 124.2, and 125 °C) samples did not crystallize during the previous cooling. Finally, the samples were crystallized isothermally at the different chosen T_c values.

3.5. Tensile Properties. The tensile tests were carried out according to the normalized procedure suggested by ASTM D 1708 for microtensile tests.[36] The tests were performed in a JJ Lloyd T5003 universal testing machine at a constant testing rate of 10 mm/min and ambient temperature (22 °C).

4. Results and Discussion

4.1. Neat HDPE Sample: van Gurp Plot and Relaxation Times. The van Gurp−Palmen plot is a very useful tool used to identify relaxing species in complex polymeric systems.[37,38] This plot (phase angle, δ, versus modulus of the complex modulus, $|G^*|$) not only serves to evaluate polydispersity effects on the linear viscoelastic response of linear polymers but also provides information on the effect of long chain branching (LCB) in single-site catalyst polymers and other model monodisperse polymers. The plot has the added advantage that no M_w normalization is needed. For linear systems, the dependence of δ on $|G^*|$ is found to rise from very small values at high values of $|G^*|$, up to the viscous limit ($\delta = 90°$) at low values of $|G^*|$. The solid lines in Figure 1 indicate the typical behavior of linear polyethylenes with different polydispersity index taken from the literature.[37,38] The neat HDPE sample is included. As it is observed, the HDPE studied here (commercial 7000F) shows the characteristic behavior of a polydisperse polyethylene ($M_w/M_n > 10$), but also exhibits an inflection at low values of $|G^*|$, which it is characteristic of materials with bimodal molecular weight distribution and molecular species with high relaxation times (including long chain branching).

4.2. Influence of Dispersed MWNTs in HDPE Melt: Linear Viscoelasticity. From literature results, one can find that the percolation threshold in polymer/nanotube composites is influenced by several factors: aspect ratio[39,40] dispersion[41] and alignment.[28,42,43] In the case of polyolefins values of the percolation threshold ranging from 0.5 to 7.5% can be found.[21−23] Percolated networks give rise to secondary "plateau" regions in the storage modulus, G', at low frequencies. The results shown in Figure 2 strongly support the absence of a percolated network in our nanocomposite, as in all the explored frequency range the storage modulus decreases and the complex viscosity decreases considerably (~30%) with a presence of 0.52 wt % of CNT. This difference is far away from the accuracy of the technique. The presence of a third component (i.e., the 0.43% of another PE, the one obtained *in situ* onto the surface of the CNT) with a lower viscosity cannot explain the reduced values of the viscoelastic properties (assuming a general mixing rule for homogeneous polymer blends). This observation is not new. Recently Zhang et al.[22] have reported a considerable decrease in both the viscosity and the modulus for a series of broad molecular weight distribution (MWD) UHMWPE/single wall CNTs (SWNT) nanocomposites in the range of compositions (0.1−1%). On the contrary, for different nanocomposites based on narrow MWD UHMWPE or conventional HDPE, they found that the samples do not suffer a drop in dynamic viscosity, but a fast and continuous increase in the modulus and viscosity as the CNT loading increases.

Zhang et al.[22] explain their findings as a consequence of the selective adsorption of the longest molecules of the broad molecular weight distribution onto the CNT surface. Because of the selective adsorption of the high molar mass species, the apparent molar mass of the polymer matrix decreases; and consequently, the modulus and viscosity decreases, as the entanglement density is reduced. This does not occur in an UHMWPE with a narrow MWD, as all the molecules are similar, and then, no clear distinction in the molecular weight between the polymer matrix before and after the adsorption of chains to CNT surface exists. In the case of conventional HDPE (with molecular weight lower than 400 kg/mol), for which neither decreased moduli nor decreased viscosity is observed, they consider the existence of a critical molecular weight of the polymer to notice the preferred adsorption mechanism. Then, why in our case we observe decreased modulus and viscosity in a matrix of HDPE? A similar explanation could apply in our case if we take into account the specific molecular characteristics of the HDPE matrix used in our composite (which possesses a bimodal distribution of molar masses), and we refer to relaxation time distribution. The idea is that the molecules with the longest relaxation times adsorb onto the nanotube surface (via van de Waals interaction).[22] Within the experimental time window the probability of the high relaxation time species to remain adsorbed on the nanotubes will be higher than that of the low relaxation time chains. The adsorbed polymer chains, especially those with the highest relaxation times, can be considered as an immobilized part on the CNT, at least for times within the experimental time window (frequency window). Thus, the polymer forming the remaining matrix will effectively have a lower average relaxation time than the unfilled polymer. Moreover a reduced entanglement density promoted by the adsorption mechanism can also occur. This would cause faster relaxation of chains thus a decrease in the storage modulus and viscosity.

The observed drop in the viscosity values at such a low concentration of filler is in agreement with recent findings

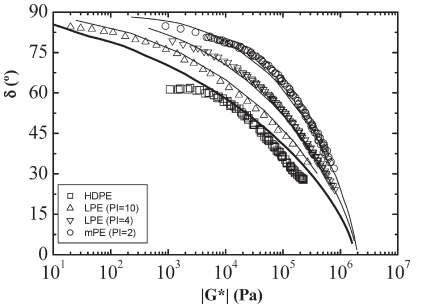

Figure 1. Van Gurp−Palmen plot at 160 °C of PE samples of different molecular weight distribution:[37,38] (○) HDPE with $M_w/M_n = 2$; (▽) HDPE with $M_w/M_n = 4$; (△) HDPE with $M_w/M_n = 10$; (□) HDPE sample employed in this work. The lines represent the behavior expected for HDPE samples with different M_w/M_n values between 2 and 20 (Gaussian distribution).

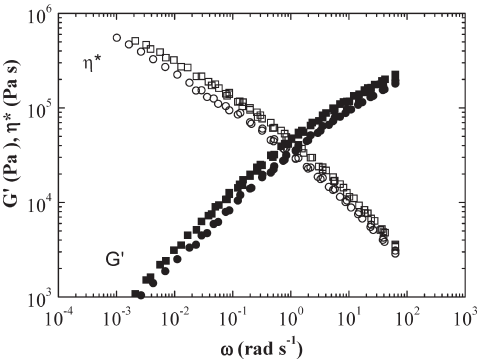

Figure 2. Storage modulus, G', and complex viscosity, $|\eta^*|$, at 160 °C of the HDPE/MWNT nanocomposite (circles) and neat HDPE (squares).

reported in other types of composites. We have compared in Figure 3 the values of the reduced complex viscosity ($\eta_{composite}/\eta_{matrix}$) versus CNT loadings taken at 160 °C and low frequency (Figure 3), with those results taken from the literature for PE/CNT nanocomposites. A clear decrease is observed in our nanocomposite, similarly to UHMWPE (broad MWD)/CNT composites. Kharchenko et al.[20] too observed on MWNT filled polypropylene that the viscosity decreases strongly with increasing shear rate, and also these nanocomposites exhibit impressively large and negative normal stress differences (ΔN). This work has emphasized the rheological properties of relatively *high aspect ratio* multiwall CNT nanocomposites (A from 300 to 400). The proposed mechanism relies on the capacity of the "struts" of the CNT network to rotate about their impingement junctions.

Mackey et al.[44,45] also reported a decreased viscosity in polystyrene filled with cross-linked polystyrenes nanoparticles. They consider that the increase in the free volume as well as certain configurational changes to the linear polymer may be responsible for reducing the viscosity. Jain et al.[46] observed a similar drop in viscosity using silica nanoparticles as filler. In polymers filled with silica, an explanation provided for the viscosity drop was the selective physical-adsorption of polymer chains onto nanoparticle surface. Independently, Maurer et al. observed preferential adsorption of high molar mass component in polydisperse UHMWPE on silica particles.[47] Accordingly, it can be stressed that the important variable controlling this process is the relaxation time distribution of the matrix.

Is important to mention that theoretical works suggest that the nature of the particle polymer interaction—attractive vs repulsive—may play a role in whether or not a viscosity reduction can take place. The molecular dynamics simulations done by Kropka et al.[48] in their studies on C60−polymer mixtures (PS, PMMA, and TMPC), showed that the dynamics of the polymer segments in the vicinity of the particle surfaces are suppressed relative to the neat polymer, and this effect results in an excess elastic fraction of polymer segments at the nanosecond time scale. Smith et al.[49] showed similar results, the viscoelastic properties of the polymer matrix were strongly perturbed by the nanoparticles and depended upon the nature of the nanoparticle−polymer interactions. For repulsive systems, a faster polymer dynamics were observed relative to the pure melt and neutral systems and were associated with a decrease in the polymer matrix density. On the other hand, in attractive interactions, the slowing of polymer dynamics observed was associated with a dramatic reduction in mobility of adsorbed polymer segments along the nanoparticle surface.

4.3. Practical Consequences of the Presence of Dispersed CNTs in HDPE Melt. *4.3.1. Processing: Capillary Flow*. It is common practice in rheology to compare the magnitude of the complex dynamic shear viscosity $|\eta^*|$, obtained by subjecting a material to a low amplitude oscillatory shear, with the shear viscosity, obtained in continuous torsion flow or even in capillary flow. The phenomenological Cox−Merz rule,[50] which often holds to a good approximation for entangled polymer fluids, does not apply to percolated CNT nanocomposites (above the threshold concentration). This finding is consistent with former observations on filled polymers[51] concentrated aqueous nanotube dispersions,[52] and clay-based nanocomposites.[53]

In Figure 4, we can observe the application of the Cox−Merz rule for the values of the oscillatory complex viscosity and torsion and capillary shear viscosity in the case of our nanocomposite. The result strongly supports the Cox−Merz

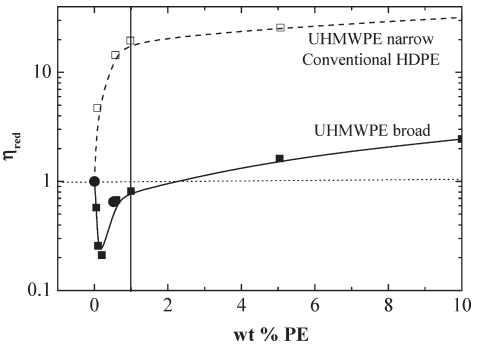

Figure 3. Comparison with literature results of reduced viscosity ($\eta_{comp}/\eta_{matrix}$) for different polyethylene/CNT composites: (●) our materials; (■) UHMWPE (broad MWD) composites;[22] (□) UHMWPE (narrow MWD) composites.[22] The solid vertical line represents the percolation threshold for the viscosity function. The dashed horizontal line represents the reduced viscosity of the matrix (an independent variable from molecular architecture).

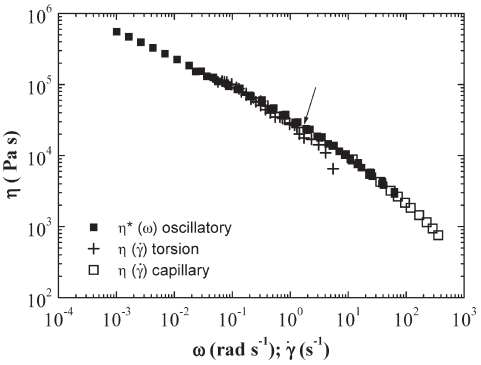

Figure 4. Application of the Cox−Merz rule for the HDPE/MWNT nanocomposite at 160 °C. The arrow indicates the onset of wall slip in torsion shear measurements. Similar results (not shown) are obtained for the neat HDPE sample.

rule (except in the case of torsion shear viscosity at high shear rates, a result likely due to slip or spurt of the material from the measuring system). This is a typical result in entangled polymer fluids and composites below the percolation threshold.

The comparison of the values obtained of the extrusion apparent shear stress, $\sigma_{w,app}$, in both neat HDPE and the nanocomposite, again results in lower values in the case of the nanocomposite (see Figure 5). The shear stress in the case of the nanocomposite is 20% lower than in the case of neat HDPE, in agreement with the idea of an increased mobility of the system as a consequence of the physical adsorption of the molecules with the highest relaxation times (viscosity) onto the CNT surface. Interestingly, the "slip-stick" distortion regime, typical of polyolefins at high shear rates, shifts to higher values of the critical shear stress and shear rate in the case of the nanocomposite. In this case the throughput-processing rate increases up to 200% the corresponding value of the neat HDPE. In general it is assumed that the distortion regimes appear at a critical value of σ_w/G, then an increased value of the critical shear stress means a decreased value of the modulus, G, as it has been shown previously in Figure 2. Once again this result is a signature of a decreased concentration of entanglements, probably due to the adsorbed layer of large molecules trapped onto the CNT surface.

The existence of these "inactive" molecules in the nanocomposite may be expected to have an impact not only in processing, but also in ultimate material properties. In fact,

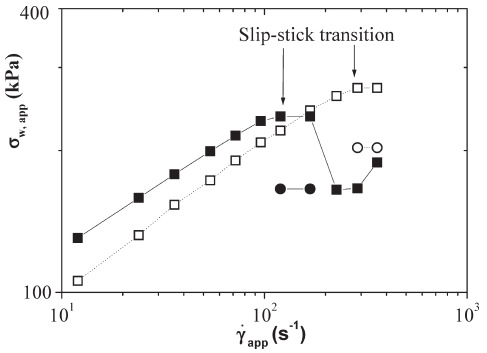

Figure 5. Flow curves obtained in capillary flow at 160 °C: (■) HDPE; (□) HDPE/MWNT nanocomposite. The arrows indicate the point at which slip-stick distortion regime starts in each case.

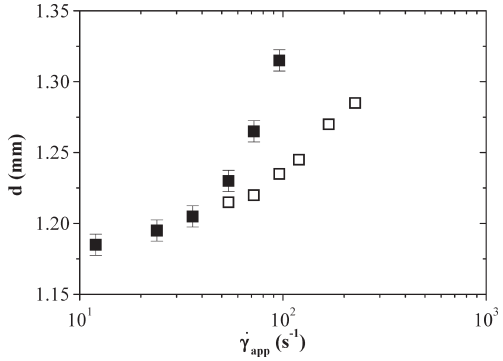

Figure 6. Extrudate swell versus apparent shear rate obtained in extrusion capillary measurements at 160 °C: (■) HDPE matrix and (□) HDPE/MWNT nanocomposite.

in section 4.3.4. below, we will report a curious behavior of the strain at yield that could be attributed to the deactivation of the longest chains that are usually present in the amorphous zones that interconnect the crystalline lamellae. The extrusion of high-molecular-mass entangled fluids such as neat HDPE matrix, normally exhibits significant die swell in extrusion. One might expect the less entangled state to lead to a change in the dimensions of the extruded jet of HDPE/MWNT nanocomposite. Figure 6 shows that the cross-section of the nanocomposite extrudate, *d*, indeed becomes significantly smaller than that corresponding to the neat HDPE sample. This means that the dimensional stability of the nanocomposite improves with respect to that observed in neat HDPE. Kharchenko et al.[20] in their studies done on polypropylene/CNT nanocomposites also observed a reduction in die swell. This study and recent contributions of the same authors[10,26] indicate that the aspect ratio of the carbon nanotubes plays a key role in processing. Specifically, for high aspect ratio of the CNT, nanocomposites exhibit remarkably large and negative normal stress differences, a rarely reported phenomenon in soft condensed matter. One might expect, based on existing models,[54] a negative normal stress to lead to a die shrinkage or little change in the dimensions of an extruded nanocomposite, as occurs in our case. For the low aspect ratio CNT/polymer nanocomposites, the apparent normal stresses are observed to be strictly positive, and then the low aspect ratio nanocomposite exhibited *die swell*.

4.3.2. Melt Elongational Properties. Also important differences have been obtained in the extensional flow curve of the materials studied as can be observed in Figure 7. The maximum tensile force obtained for each sample is the "melt strength" or the force at rupture of the extruded filament,

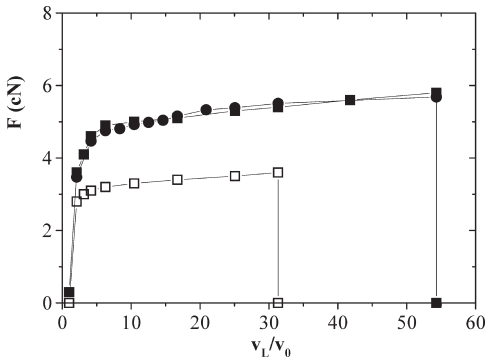

Figure 7. Tensile force versus drawn ratio in the melt spinning experiment at 160 °C: (■, ●) HDPE matrix and (□) HDPE/MWNT nanocomposite. Reliability in the results obtained from these measurements are demonstrated in the case of HDPE sample (two independent measurements).

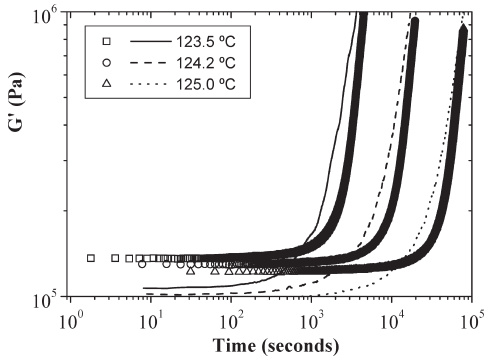

Figure 8. Isothermal crystallization monitored by the time evolution of the storage modulus, G', at different temperatures (123.5 °C, 124.2, and 125.0 °C) of HDPE matrix (symbols) and HDPE/MWNT nanocomposite (lines) at constant strain (γ = 0.15%) and frequency (1 Hz).

under the conditions established in the experimental part. A high tensile force, i.e., high tensile stress and viscosity, characterizes the neat HDPE sample. The equivalent value of the tensile stress rupture for this material is 5 MPa, slightly higher than the values obtained for LLDPE, HDPE, and LDPE (0.5, 0.8, and 2 MPa, respectively).[55] Notwithstanding, it should be noted that these values are strongly dependent on the experimental conditions used and setup features. The HDPE/MWNT nanocomposite shows lower values of the tensile force at the same draw ratio. The filaments also break at a lower value of the draw ratio than in the case of the neat HDPE matrix, and the critical stress for rupture is also lower. The result indicates that the elongational viscosity of the nanocomposite is also lower than that corresponding to the neat HDPE sample. The presence of MWNT causes decreased values of elongational properties and tensile stress at break, probably due to the lower number of entanglements caused by the selective adsorption of the longer chains onto nanotube surface.

4.3.3. Crystallization. In Figure 8, we can observe the evolution of the storage modulus for both neat HDPE and the HDPE/MWNT nanocomposite sample at different crystallization temperatures. This figure shows that the presence of the CNT in the composite causes the onset of crystallization to occur earlier. Also a slightly different kinetics of the process is observed. The induction time for the onset of crystallization has been estimated when a change in G' of 1% takes place. In Figure 9a, we can observe the calculation of the induction time from the reduced storage modulus, defined as $G_{red} = G'(t)/G'(t=0)$. Figure 9b shows that the onset of the crystallization process is faster by a factor of 3 in the

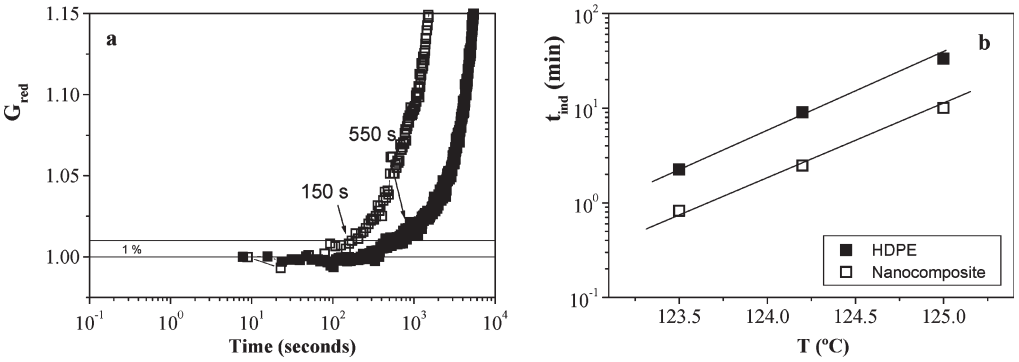

Figure 9. (a) Definition of the time for the onset of the crystallization process for (■) HDPE matrix and (□) HDPE/MWNT nanocomposite at a crystallization temperature of 124.2 °C. (b) Induction time versus crystallization temperature from the G' time evolution: (■) HDPE matrix and (□) HDPE/MWNT nanocomposite.

Table 1. Crystallization Temperatures, Melting Temperatures, Enthalpies and Crystallization Percentages Determined during Cooling and Subsequent Heating DSC Scans

sample	$T_{m\ onset}$ [°C]	$T_{m\ peak}$ [°C]	ΔH_m [J/g]	$T_{c\ onset}$ [°C]	$T_{c\ peak}$ [°C]	ΔH_c [J/g]	X_c [%]
neat HDPE	121.7	131.8	173.8	119.5	116.5	191.9	59
HDPE/MWNT nanocomposite	119.7	131.3	182.9	120.2	117.6	196.9	62

nanocomposite than in the neat HDPE matrix. Considering that the applied low strain (0.15%) does not have an effect on the crystallization process, the enhancement of nucleation/crystallization on addition of CNT suggests that the emerging structure is likely a result of the crystallization of the polymer chains onto the nanotube surface, where the CNT surface acts as a nucleation site for PE chains to crystallize.

The DSC results obtained by both standard and isothermal experiments corroborate the nucleating effect of the MWNT on the HDPE. Such nucleating effects have been previously reported in the literature.[33,34] Table 1 summarizes data extracted from cooling and heating DSC scans. The nucleating effect is detected by the increase in crystallization temperature of 1 °C, a small but significant number in view of the high nucleation density of polyethylene. The melting temperature and crystallinity were not altered by the presence of the MWNTs. In dynamic scans nevertheless melting curves after SSA treatment exhibit differences between neat polymer and nanocomposites.[34]

When isothermal DSC experiments were performed (see Figure 10) at the same crystallization temperatures employed in Figure 8, it was found that not only the crystallization process starts in the nanocomposite sample earlier than in the neat HDPE but the entire crystallization process occurs faster.

The crystallization kinetics was described in terms of the Avrami equation, a common tool to describe overall isothermal crystallization (including nucleation and growth). The Avrami equation can be written as[56,57]

$$1 - V_c(t) = \exp(-kt^n) \qquad (1)$$

where V_c is the relative transformation volume fraction at the crystallization time t; k is the overall crystallization rate constant, which is a function of nucleation and growth, and n is the Avrami index. The Avrami index is a complex exponent whose value is related to the dimensionality of the growing crystals and to the time dependence of nucleation. In order to fit the experimental data to the Avrami equation, we closely followed the procedure given in ref 58.

Figure 11 shows how the crystallization half-time (an experimental measure of the inverse of the overall relative crystallization rate) depends on the crystallization temperature. In the nanocomposite case the times to achieve 50% of

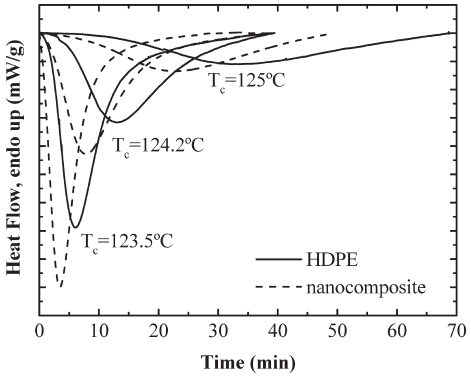

Figure 10. Isothermal crystallization monitored by DSC at different isothermal crystallization temperatures (123.5, 124.2, and 125.0 °C) for neat HDPE and the HDPE/MWNT nanocomposite sample.

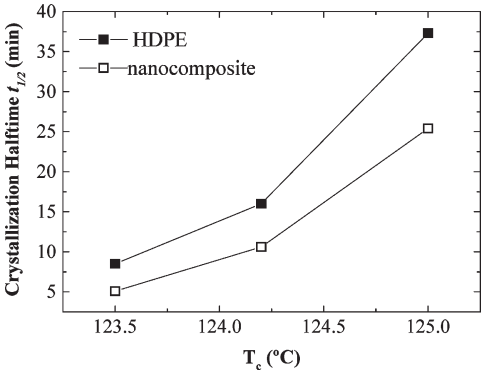

Figure 11. Crystallization halftime versus crystallization temperature for neat HDPE and HDPE/MWNT nanocomposite system.

Table 2. Avrami Index (n), Overall Crystallization Rate Constant (k), and Experimentally Determined Half-Crystallization Time Obtained during Isothermal Crystallization of Neat HDPE and HDPE/MWNT Nanocomposite

		HDPE		HDPE/MWNT nanocomposite		
T_c [°C]	N	K [min^{-n}]	$t_{1/2}$ [min^{-1}]	n	K [min^{-n}]	$t_{1/2}$ [min^{-1}]
123.5	3.3	8.9×10^{-4}	8.5	2.6	1.2×10^{-2}	5.1
124.2	3.6	5.6×10^{-5}	16.0	2.9	9.7×10^{-4}	10.6
125.0	3.6	1.6×10^{-6}	37.3	2.9	5.0×10^{-5}	25.4

Table 3. Mechanical Properties of Neat HDPE and HDPE/MWNT Nanocomposite

sample	E [MPa]	σ_y [MPa]	ε_y [%]	σ_b [MPa]	ε_b [%]	tenacity [KJ/m^3]
neat HDPE	334 ± 66	22 ± 0.9	27 ± 3	20 ± 2	500 ± 109	8 ± 2
HDPE/MWNT nanocomposite	610 ± 51	23 ± 0.4	11 ± 1	21 ± 3	450 ± 98	8 ± 2

the conversion to the crystalline state are always shorter than for neat HDPE and the difference is larger at lower supercoolings. This is consistent with previous results on the crystallization kinetics of the neat HDPE/MWNT master batch.[33,34]

Table 2 lists relevant parameters obtained from the isothermal crystallization experiments by DSC and the Avrami fits. Larger values of the overall crystallization rate constant k were obtained for the nanocomposite with respect to neat HDPE, a result which is fully consistent with the trend obtained in the experimentally determined half-crystallization times. The Avrami index is generally close to 3 and slightly lower values were obtained for the nanocomposite. These Avrami indexes indicate for both cases that instantaneously nucleated spherulites are being produced. More dramatic reductions in Avrami index can be obtained if the CNT load is increased to very large concentrations, since the morphology can also be significantly altered by confinement effects.

4.3.4. Mechanical Behavior. Table 3 presents values of the representative mechanical properties obtained by uniaxial tensile testing. The reinforcement obtained in rigidity is probably the most outstanding result obtained since adding only 0.54 wt % of MWNT causes an increase in elastic modulus of about 100%. This is expected since MWNT have elastic modulus values on the range 270−950 GPa.[58,59] Even though the modulus increases, the tenacity (area under the stress−strain curve) is not compromised, and the material is still as ductile as neat HDPE. This is an attractive mechanical behavior since with the use of conventional fillers an increase in rigidity is usually accompanied by a loss in ductility (lower tenacity and lower elongation at break). The good mechanical properties are also a sign of good dispersion and adequate adhesion between the nanofiller and the matrix.

Another interesting aspect is that the strain at yield (ε_y) has been substantially reduced in the HDPE/MWNT nanocomposite as compared to neat HDPE, as can be clearly seen in Figure 12, where typical experimental curves are shown, and in Table 3 where the mean values for this property are listed.

The mechanism of neck formation is related to localized shear yielding. In the case of semicrystalline polymers, the plastic deformation that characterizes the yielding process has been described in terms of the slip of crystalline blocks together with the deformation of the defective intercrystalline regions followed by homogeneous shear deformation of the crystal blocks.[60−66] In this process, the tie molecules (which link crystal block regions by passing though the intervening amorphous layers) play an important role. We have shown above rheological evidence suggesting that a fraction of the long HDPE molecules are adsorbed at the CNT surface and as a consequence the entanglement density in the material is lower thereby producing lower viscosity and elasticity in the molten state. It is then conceivable that once the polymer solidifies the number of tie molecules is also lower as compared to those in neat HDPE. This decreased number of tie chains could be responsible for the increased sensitivity of the nanocomposite to undergo yielding at lower deformations than neat HDPE.

Finally, the tensile properties at break did not experience any change (HDPE versus nanocomposite) within the

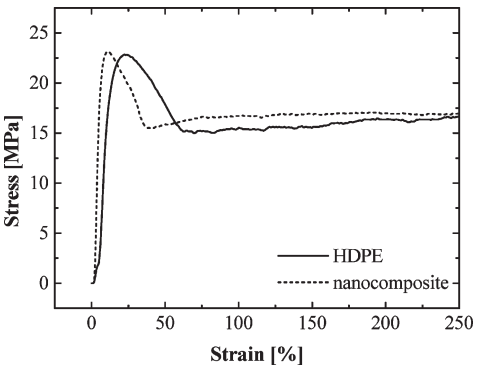

Figure 12. Engineering stress−strain curve limited to 250% deformation in order to highlight the yielding region for neat HDPE and the HDPE/MWNT nanocomposite.

experimental error of the measurements. In summary, in the HDPE/MWNT nanocomposite examined here, we have obtained a significant increase in tensile modulus without loosing tenacity. In the literature other tendencies have been obtained in similar systems.[58,67] McNally et al.[21] prepared PE/MWNT nanocomposites with compositions ranging from 0.1 to 10 wt % by melt blending and reported a poor stress transference between the matrix and the filler, as deduced from the results obtained by static and dynamic mechanical properties. They argue that the mechanism of reinforcement is based on interfacial interactions between the matrix and the filler and not by a fibrillar percolation network as proposed by Zou et al.[68] In both cases, the PE/CNT nanocomposites were prepared by melt mixing but in this case the MWNT had a previous superficial treatment with SiO_2. Additionally, in the McNally studies the tenacity was reduced when the CNT content was increased.

Recently, Kanagaraj et al.[69] studied the mechanical and tribological properties of HDPE reinforced with 0.11, 0.22, 0.33, and 0.44 wt % of chemically treated MWNT by melt blending. The CNTs were functionalized with different functional groups like carboxyl, carbonyl, hydroxyl, and others. According to their results, the yield stress was not modified and the elastic modulus was increased up to 22%.

5. Conclusions

The linear viscoelastic fingerprint of the neat HDPE sample suggests that this polymer has a fraction of molecules with very high relaxation times, a fact consistent with a bimodal molecular weight commercial HDPE sample. The nanocomposite is characterized by lower values of the viscosity and the shear modulus in the frequency range applied. This behavior has been observed in nanocomposites in which an adsorption of a fraction (that with the highest molecular weight or relaxation time) of the polymer chains is considered. The adsorption process promotes that this fraction of molecules becomes "inactive" (unentangled) within the matrix, remaining immobilized onto the surface of the nanotubes and not contributing to the viscosity or to the average relaxation time of the system. The existence of this fraction of unentangled/adsorbed chains onto the CNT surface gives rise to some interesting phenomena in processing: (i) lower values of the shear stress in extrusion and a delay of the distortion regime to higher shear stresses and rates (improvement of processability); (ii) lower values of the extrudate swell, or in other words, an

improved dimensional stability of the materials after processing; (iii) lower values of the melt strength, draw ratio and viscosity in elongational flow; (iv) enhanced crystallization kinetics probed by rheometry and DSC, suggesting that the CNTs act as nucleating agents for polymeric chains. Additionally, the presence of this peculiar interface apparently does not only influence the molten state but also provokes interesting effects in the mechanical properties of the polymer, where increases of 100% in elastic modulus were observed in the HDPE/MWNT nanocomposite without loosing the ductility present in neat HDPE.

Acknowledgment. We would like to thank the MEC (Project MAT2006-0400), and CSIC (Project PIE-200850I072) for financial support. The Venezuelan team acknowledges support from the Decanato de Investigación y Desarrollo (DID) though Grant DID-GID-02. CIRMAP thanks Nanocyl S.A. (Sambreville, Belgium) for kindly providing the carbon nanotubes. This work was partially financially supported by "Région Wallonne" and European Community (FEDER, FSECIRMAP thanks the "Belgian Federal Government Office Policy of Science (SSTC)" for general support in the frame of the PAI-6/27.

References and Notes

(1) Moniruzzaman, M.; Winey, K. I. *Macromolecules* **2006**, *39*, 5194–5205.
(2) Bredeau, S.; Peeterbroeck, S.; Bonduel, D.; Alexandre, M.; Dubois, Ph *Polym. Int*. **2008**, *57*, 547–553.
(3) Knauert, S. T.; Douglas, J. F.; Starr, F. W. *J. Polym. Sci., Part B: Polym. Phys*. **2007**, *45*, 1882–1897.
(4) Starr, F. W.; Schroder, T. B.; Glotzer, S. C. *Phys. Rev. E* **2001**, *64*, 021802/1–021802/5.
(5) Starr, F. W.; Schroder, T. B.; Glotzer, S. C. *Macromolecules* **2002**, *35*, 4481–4492.
(6) Kairn, T.; Daivis, P. J.; Ivanov, I.; Bhattacharya, S. N. *J. Chem. Phys*. **2005**, *123*, 194905/1–194905/7.
(7) Seok, Y.; Ryoun, J. *Korea-Australian Rheol. J*. **2004**, *16*, 201–212.
(8) Cipiriano, B. H.; Kashiwagi, T.; Raghavan, S. R.; Yang, Y.; Grulke, E. A.; Yamamoto, K.; Shields, J. R.; Douglas, J. F. *Polymer* **2007**, *48*, 6086–6096.
(9) Wu, D. F.; Wu, L.; Zhang, M.; Zhao, Y. L. *Polym. Degrad. Stab*. **2008**, *93*, 1577–1584.
(10) Song, Y. *Polym. Eng. Sci*. **2006**, *46*, 1350–1357.
(11) Abdalla, M.; Dean, D.; Robinson, P.; Nyairo, E. *Polymer* **2008**, *49*, 3310–3317.
(12) Seyhan, A. T.; Gojny, F. H.; Tanoglu, M.; Schulte, K. *Eur. Polym. J*. **2007**, *43*, 2836–2847.
(13) Wu, D. F.; Wu, L.; Zhang, M. *J. Polym. Sci., Part B: Polym. Phys*. **2007**, *45*, 2239–2251.
(14) Wu, D.; Wu, L.; Zhang, M.; Wu, L. *Eur. Polym. J*. **2007**, *43*, 1635–1644.
(15) Wu, D.; Wu, L.; Sun, Y.; Zhang, M. *J. Polym. Sci., Part B: Polym. Phys*. **2007**, *45*, 3137–3147.
(16) Hu, G.; Zhao, C.; Zhang, S.; Yang, M.; Wang, Z. *Polymer* **2006**, *47*, 480–488.
(17) Mitchell, C. A.; Bahr, J. L.; Arepalli, S.; Tour, J. M.; Krishnamoorti, R. *Macromolecules* **2002**, *35*, 8825–8830.
(18) Potschke, P; Abdel-Goad, M.; Alig, I.; Dudkin, S. M.; Lellinger, D. *Polymer* **2004**, *45*, 8863–8870.
(19) Du, F.; Scogna, R. C.; Zhou, W.; Brand, S.; Fischer, J. E.; Winey, K. I. *Macromolecules* **2004**, *37*, 9048–9055.
(20) Kharchenko, S. B.; Douglas, J. F.; Obrzut, J.; Grulke, E. A.; Migler, K. B. *Nat. Mater*. **2004**, *3*, 564–568.
(21) McNally, T.; Potschke, P.; Halley, P.; Murphy, M.; Martin, D.; Bell, S. E. J.; Brennan, G. P.; Bein, D.; Lemoine, P.; Quinn, J. P. *Polymer* **2005**, *46*, 8222–8232.
(22) Zhang, Q.; Lippits, D.; Rastogi, S. *Macromolecules* **2006**, *39*, 658–666.
(23) Zhang, Q.; Rastogi, S.; Chen, D.; Lippits, D.; Lemstra, P. J. *Carbon* **2006**, *44*, 778–785.
(24) Kota, A. K.; Cipriano, B. H.; Duesterberg, M. K.; Gershon, A. L.; Powell, D.; Raghavan, S. R.; Bruck, H. A. *Macromolecules* **2007**, *40*, 7400–7406.
(25) Potschke, P.; Pegel, S.; Claes, M.; Bonduel, D. *Macromol. Rapid Commun*. **2008**, *29*, 244–251.
(26) Xu, D. H.; Wang, Z. G.; Douglas, J. F. *Macromolecules* **2008**, *41*, 815–825.
(27) Potschke, P.; Fornes, T. D.; Paul, D. R. *Polymer* **2002**, *43*, 3247–3255.
(28) Du, F.; Fisher, J. E.; Winey, K. I. *J. Polym. Sci., Part B: Polym Phys*. **2003**, *41*, 3333–3338.
(29) Abdalla, M.; Dean, D.; Adibempe, D.; Nyairo, E.; Robinson, P.; Thompson, G. *Polymer* **2007**, *48*, 5662–5670.
(30) Valentino, O.; Sarno, M.; Rainone, N. G.; Nobile, M. R.; Ciambelli, P.; Neitzert, H. C.; Simón, G. P. *Physica E* **2008**, *40*, 2440–2445.
(31) Xiao, K. Q.; Zhang, L. C.; Zarudi, I. *Compos. Sci. Technol*. **2007**, *67*, 177–182.
(32) Mathot, V. B. F. In *Calorimetry and Thermal Analysis of Polymers*; Mathot, V. B. F., Ed.; Hanser Publishers: Munich, Vienna, and New York, 1994.
(33) Trujillo, M.; Arnal, M. L.; Müller, A. J.; Laredo, E.; Bredeau, St.; Bonduel, D.; Dubois, Ph. *Macromolecules* **2007**, *40*, 6268–6276.
(34) Trujillo, M.; Arnal, M. L.; Müller, A. J.; Bredeau, St.; Bonduel, D.; Dubois, Ph.; Hamley, I. W.; Castelletto, V. *Macromolecules* **2008**, *41*, 2087–2095.
(35) Bonduel, D.; Bredeau, S.; Alexandre, M.; Monteverde, F.; Dubois, Ph. *J. Mater. Chem*. **2007**, *17*, 2359–2366.
(36) *ASTM D 1708-02: Standard Test Method for Tensile Properties of Plastics By Use of Microtensile Specimens*; ASTM International: West Conshohocken, PA, 2002, Vol. 8.01.
(37) Trinkle, S.; Walter, P.; Friedrich, C. *Rheol. Acta* **2002**, *41*, 103–113.
(38) Trinkle, S.; Friedrich, C. *Rheol. Acta* **2001**, *40*, 322–328.
(39) Bryning, M. B.; Islam, M. F.; Kikkawa, J. M.; Yodh, A. G. *Adv. Mater*. **2005**, *17*, 1186–1191.
(40) Bai, J. B.; Allaoui, A. *Composites, Part A* **2003**, *34A*, 689–694.
(41) Barrau, S.; Demont, P.; Perez, E.; Peigney, A.; Laurent, C.; Lacabanne, C. *Macromolecules* **2003**, *36*, 9678–9680.
(42) Du, F.; Fischer, J. E.; Winey, K. I. *Phys. ReV. B: Condens. Matter* **2005**, *72*, 121404/1–121404/4.
(43) Haggenmueller, R.; Gommans, H. H.; Rinzler, A. G.; Fischer, J. E.; Winey, K. I. *Chem. Phys. Lett*. **2000**, *330*, 219–225.
(44) Mackay, M. E.; Dao, T. T.; Tuteja, A.; Ho, D. L.; Van Horn, B.; Kim, H.-C.; Hawker, C. J. *Nat. Mater*. **2003**, *2*, 762–766.
(45) Tuteja, A.; Mackay, M. E.; Hawker, C. J.; Horn, B. V. *Macromolecules* **2005**, *38*, 8000–8011.
(46) Jain, S.; Goossens, J. G. P.; Peters, G. W. M.; Van Duin, M.; Lemstra, P. J. *Soft Matter* **2008**, *4*, 1842–1854.
(47) Maurer, F. H. J.; Schoffeleers, H. M., Kosfeld; R., Uhlenbroich, T. In *Progress in Science and Engineering of Composites*; Hayashi, T., Kawata, K., Umekawa, S., Eds.; ICCM-IV: Tokyo, 1982; p 803.
(48) Kropka, J. M.; Garcia, V.; Green, F. *Nano Lett*. **2008**, *8*, 1061–1065.
(49) Smith, G. D.; Bedrov, D.; Li, L.; Byutner, O. *J. Chem. Phys*. **2002**, *117*, 9478–9489.
(50) Cox, W. P.; Merz, E. H. *J. Polym. Sci*. **1958**, *28*, 619–622.
(51) Al-Hadithi, T. S. R.; Barnes, H. A.; Walters, K. *Colloid Polym. Sci*. **1992**, *270*, 40–46.
(52) Kinloch, I. A.; Roberts, S. A.; Windle, A. H. *Polymer* **2002**, *43*, 7483–7491.
(53) Ren, J. X.; Krishnamoorti, R. *Macromolecules* **2003**, *36*, 4443–4451.
(54) Tanner, R. I. In *Engineering Rheology*; Oxford University Press: New York, 2000.
(55) Bernnat, A. *Polymer melt reologhy and the rheotens test* Ph.D. Thesis, Universitat Stuttgart, **2000** (http://elib.uni-stuttgart.de/opus/volltexte/2002/992/pdf/diss_bn.pdf).
(56) Mandelkern, L. In *Physical Properties of Polymers*; 3rd ed. Mark, J. E., Eds.; Cambridge University Press: Cambridge, U.K., 2004.
(57) Lorenzo, A. T.; Arnal, M. L.; Albuerne, J.; Müller, A. J. *Polym. Test*. **2007**, *26*, 222–231.
(58) Yu, M. F.; Lourie, O.; Dyer, M. J.; Moloni, K.; Kelly, T. F.; Ruoff, R. S. *Science* **2000**, *287*, 637–640.
(59) Yu, M. F.; Files, B. F.; Arepalli, S.; Ruoff, R. S. *Phys. Rev. Lett*. **2000**, *84*, 5552–5555.
(60) Bowden, P. B.; Young, R. J. *J. Mater. Sci*. **1974**, *9*, 2034–2051.
(61) Lin, L.; Argon, A. S. *J. Mater. Sci*. **1994**, *29*, 294–323.
(62) Crist, B.; In *Materials Science and Technology, A Comprehensive Treatment. Structure and Properties of Polymers*, 1st. Ed.; Cahn, R. W., Haasen, P., Kramer, E. J., Eds.; VCH Publishers Inc.: New York, 1993; Vol. 12, p 428.

(63) Popli, R.; Mandelkern, L. *J. Polym. Sci., Polym. Phys. Ed.* **1987**, *25*, 441–483.
(64) Flory, P. J.; Yoon, D. Y. *Nature* **1978**, *272*, 226–239.
(65) Wignall, G. D.; Wu, W. *Polym. Commun.* **1983**, *24*, 354–359.
(66) Annis, B. K.; Strizak, J.; Wignall, G. D.; Alamo, R. G.; Mandelken, L. *Polymer* **1996**, *37*, 137–140.
(67) Tang, W.; Santare, M. H.; Advani, S. G. *Carbon* **2003**, *41*, 2779–2785.
(68) Zou, Y.; Feng, Y.; Wang, L.; Liu, X. *Carbon* **2004**, *42*, 271–277.
(69) Kanagaraj, S.; Varanda, F. R.; Zhil'tsova, T. V.; Oliveira, M. S. A.; Simoes, J. A. O. *Compos. Sci. Technol.* **2007**, *67*, 3071–3077.